ELSEVIER

Journal of Nuclear Materials 271&272 (1999) 11–14

journal of nuclear materials

Radiation-induced amorphization and recrystallization of α-SiC single crystal

K. Kawatsura [a,*], N. Shimatani [a], T. Igarashi [a], T. Inoue [a], N. Terazawa [a], S. Arai [a], Y. Aoki [b], S. Yamamoto [b], K. Narumi [b], H. Naramoto [b], Y. Horino [c], Y. Mokuno [c], K. Fujii [c]

[a] *Department of Chemistry and Materials Technology, Faculty of Engineering and Design, Kyoto Institute of Technology, Goshokaido-cho, Matsugasaki, Sakyo-ku, Kyoto 606-8585, Japan*

[b] *Department of Materials Development, Japan Atomic Energy Research Institute, Takasaki, Gunma 370-1208, Japan*

[c] *Division of Materials Physics, Osaka National Research Institute, AIST, Ikeda, Osaka 563, Japan*

Abstract

Single crystals of α-SiC were irradiated with 1.0 MeV Ni and 1.3 MeV Au ions at room temperature. The dose dependence of the amorphization and the thermal annealing behavior of the induced damage were studied mainly by using Rutherford backscattering spectroscopy with channeling (RBS-C), and partly by using laser Raman scattering spectroscopy (LRSS) and scanning electron microscopy (SEM). From the RBS-C measurement, an empirical relationship between the amorphization dose and the atomic number Z was deduced. From thermal annealing of Ni implanted samples, drastic recrystallization of the amorphized layer and diffusion of implanted Ni atoms toward the Sic surface were observed at 1500°C annealing. © 1999 Elsevier Science B.V. All rights reserved.

1. Introduction

Because of its extreme hardness, high temperature stability, high thermal conductivity, chemical inertness and high temperature semiconductor properties, silicon carbide (SiC) is a prospective modern material for optoelectronics and semiconductor technology. It is also proposed as a structural material for fusion reactors in a harsh environment. Since the late 1960s, implantation and annealing behavior of SiC single crystals have been studied [1–13], because post-implantation heat treatments were necessary in order to electrically activate the implanted ions. This work led to the question of the annealing behavior of lattice damage that is introduced by the implantation process. It is found that the recrystallization temperature varies between 750°C and 1700°C. This may have been due to different doses, ion species, implantation temperatures, and so on. Therefore, it seems worthwhile to undertake a systematic study of the annealing behavior of SiC.

In the present work, we investigated the dose dependence of the amorphization of α-SiC during the ion implantation of 1.0 MeV Ni and 1.3 MeV Au at room temperature and the thermal annealing behavior of the radiation-induced defects and the implanted atoms.

2. Experimental

The α-SiC single crystals employed in this experiment were obtained from Taiheiyorundum Co., which were synthesized by the Acheson method. The polytype of the SiC single crystal before ion implantation was confirmed to be 6H type by laser Raman scattering spectroscopy (LRSS). The 6H-type α-SiC(0 0 0 1) samples were implanted with 1.0 MeV Ni and 1.3 MeV Au ions at room temperature using the 3 MV tandem accelerator of the Japan Atomic Energy Research Institute in Takasaki (JAERI-Takasaki). Ni and Au ion doses were in the range of 1.8×10^{13}–1.8×10^{17} and 3.6×10^{12}–3.6×10^{14} cm^{-2}, respectively, with a current density of 0.5–1.0 μA

* Corresponding author. Tel.: +81 75 724 7507; fax: +81 75 724 7210; e-mail: kawatura@ipc.kit.ac.jp

0022-3115/99/$ – see front matter © 1999 Elsevier Science B.V. All rights reserved.
PII: S 0 0 2 2 - 3 1 1 5 (9 8) 0 0 7 2 6 - 0

cm^{-2}. The unimplanted region of the samples with an Al foil mask was used for reference. The thermal annealing was done in a gas flow of argon up to temperatures of 1500°C for 2 h. Before and after thermal annealing, the surface for each sample was examined by using scanning electron microscopy (SEM). The formation of atomic defects after implantation and the remaining lattice disorder after thermal annealing were analyzed by Rutherford backscattering spectroscopy with channeling (RBS-C) [14]. RBS-C measurements using 1.6 MeV $^4He^+$ ions were performed at the 2 MV van de Graaff accelerator of the Osaka National Research Institute in Ikeda. The experiments with a beam of 3.0 MeV $^4He^+$ ions were performed at the 3 MV electrostatic accelerator of the JAERI-Takasaki.

3. Results and discussion

3.1. Relation between atomic number and ion dose for amorphization

Curves (a), (b) and (c) in Fig. 1 show the ⟨0 0 0 1⟩ aligned backscattering spectra of 1.6 Me V $^4He^+$ ions from the 1.0 MeV Ni implanted α-SiC single crystal with ion doses for unimplanted, 1.8×10^{14} and 5.4×10^{14} cm^{-2} at room temperature, respectively. As a reference, the random oriented spectrum from the unimplanted region of the same α-SiC sample is also shown in Fig. 1(d). The aligned spectrum in Fig. 1(b) shows larger aligned yields than those from the unimplanted sample, which mean the lattice disorder is induced in the α-SiC single crystal due to radiation damage by Ni ion implantation. Now we define the χ_{min} which measures the degree of disorder of α-SiC sample is the ratio of the ⟨0 0 0 1⟩ aligned yields to the random ones. In this paper, "amorphization" is defined when the value of χ_{min} reaches unity at a given fluence of incident ions. In Fig. 1(c), it is found that the value of χ_{min} for Si sublattice from the surface to the depth of 700 nm reaches 1.0 after Ni ion implantation of a dose of 5.4×10^{14} cm^{-2}.

Fig. 2(a), (b) and (c) shows the ⟨0 0 0 1⟩ aligned backscattering spectra of 1.6 MeV $^4He^+$ ions from the 1.3 MeV Au implanted α-SiC single crystal with ion doses for unimplanted, 3.6×10^{13} and 3.6×10^{14} cm^{-2} at room temperature, respectively. As a reference, the random oriented spectrum from the unimplanted region of the same α-SiC sample is also shown in Fig. 2(d). It is also found for 1.3 MeV Au ion implantation that the value of χ_{min} for Si sublattice from the surface to the depth of 400 nm reaches 1.0 at a dose of 3.6×10^{14} cm^{-2}, which is a lower dose than that for Ni ion implantation. No peak was indicated in laser Raman spectra for both of the amorphized samples implanted with 1.0 MeV Ni and 1.3 MeV Au ions.

Fig. 3 shows the amorphization dose as a function of atomic number Z together with other data [1,4–6,8,9]. The simple empirical relationship is obtained as follows

$$\Phi c = (2.2 \times 10^{16})/Z^{1.3}\ cm^{-2}, \tag{1}$$

where Φ_c is the amorphization dose with ion irradiation at room temperature. This simple relationship between the critical dose for amorphization and atomic number of implanted ions reproduced rather well previous experimental data as shown in Fig. 3. Amorphization takes places more easily in covalent crystals such as Si and SiC than in metallic or ionic crystals. During ion implantation, target atoms are displaced from lattice sites to interstitial ones in any type of crystal among

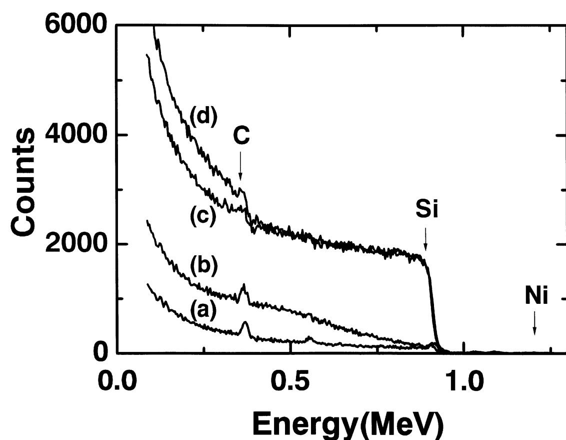

Fig. 1. Backscattering spectra of 1.6 MeV $^4He^+$ from α-SiC(0 0 0 1) single crystal implanted with 1.0 MeV Ni ions at room temperature: (a) aligned (virgin); (b) aligned (1.8×10^{14} cm^{-2}); (c) aligned (5.4×10^{14} cm^{-2}); (d) random (virgin) direction.

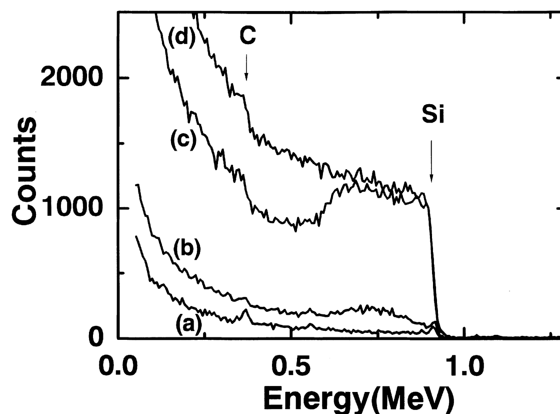

Fig. 2. Backscattering spectra of 1.6 MeV $^4He^+$ from α-SiC(0 0 0 1) single crystal implanted with 1.3 MeV Au ions at room temperature: (a) aligned (virgin); (b) aligned (3.6×10^{13} cm^{-2}); (c) aligned (3.6×10^{14} cm^{-2}); (d) random (virgin) direction.

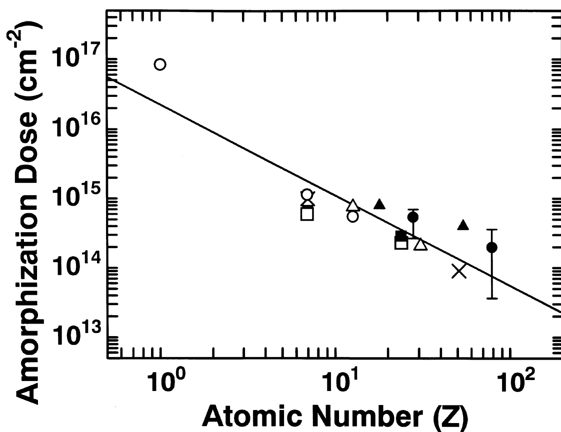

Fig. 3. The critical dose for amorphization in SiC crystal at room temperature irradiation as a function of the atomic number, Z. ●: present experimental results for Ni and Au. ×: N and Sb (Hart et al. [1]). ■: N and Cr (Williams et al. [4]. ○: H, N and Al (Spitznagel et al. [5]. □: N and Cr (McHargue et al. [5]). △: Al and Ga (Chechenin et al. [10]. ▲: Ar and Xe (Föhl et al. [9]).

these crystals. In the metallic and ionic crystals, bonding between atoms is isotropic, the displaced atoms are recovered to the lattice positions smoothly. In the covalent crystal like SiC, it needs some activation energy and orientation between atoms to form the covalent bond again. So, amorphization of SiC crystal during ion implantation depend on strongly irradiation temperature. Now, it is desirable to obtain the experimental data for low Z atoms and temperature dependence for amorphization in SiC single crystals.

3.2. Thermal annealing of induced defects and implanted atoms

The thermal annealing behavior was investigated for 1.0 MeV Ni implanted α-SiC, especially in detail of the sample of the highest dose of 1.8×10^{17} cm^{-2} at room temperature, using a 3.0 MeV $^{4}He^{+}$ beam from the 3 MV electrostatic accelerator of the JAERI-Takasaki to detect and separate the Ni spectra from those of Si and C atoms. The RBS-C measurements before thermal annealing indicate that the 1.8×10^{17} cm^{-2} implanted sample shows $\chi_{min} = 1.0$ from the surface to a depth of 900 nm. It is much deeper than 700 nm for 5.4×10^{14} cm^{-2} implanted samples (see Fig. 1(c)) as the amorphization depth depends strongly on the irradiated ion dose [8,12].

After thermal annealing at 500°C and 1000°C for 2 h in the argon ambient, the RBS-C spectra did not change from those of the as-implanted sample. Previously we have already found SiO_2 layer formation of 25 nm thickness on the α-SiC surface after 1200°C annealing for 2 h [15], so we have skipped the 1200°C annealing in the present experiment. During 1500°C annealing, recrystallization proceeded drastically from the interface between the amorphous layer and the single crystal phase to the surface. For example, the whole amorphous layer of 700 nm thickness was smoothly recrystallized from the interface to the surface for the low dose sample. On the other hand, for the highest one, the recrystallization was not completed for 2-hour annealing. Fig. 4 shows the RBS-channeling spectra of 3.0 MeV $^{4}He^{+}$ ions from an α-SiC crystal with aligned and random orientations after the 1500°C annealing for 2 h. During the 1500°C annealing, the explosive recrystallization of the whole amorphous layer occurs from the interface to the surface, and implanted Ni atoms start to diffuse toward the surface (see Fig. 5). From Fig. 4 it is deduced that the value of χ_{min} decreases to 0.2 at the surface due to recrystallization with a small amount of lattice disorder. A small step, however, is found at a depth of 500 nm, where the amount of Ni atoms was highly dense as implanted. This suggests that a defect layer with a high defect concentration exists at this depth in the recrystallized layer.

The previous results suggested that recrystallization starts epitaxially from the interface between the amorphous layer and the bulk crystal [7,12]. Present results also confirmed this mechanism for recrystallization during thermal annealing. We have performed the 1500°C annealing once more and then found that it had to take for 4 h for the complete recrystallization. The spectra by LRSS showed only the peaks from the 6H polytype as same as the virgin crystal. However, the

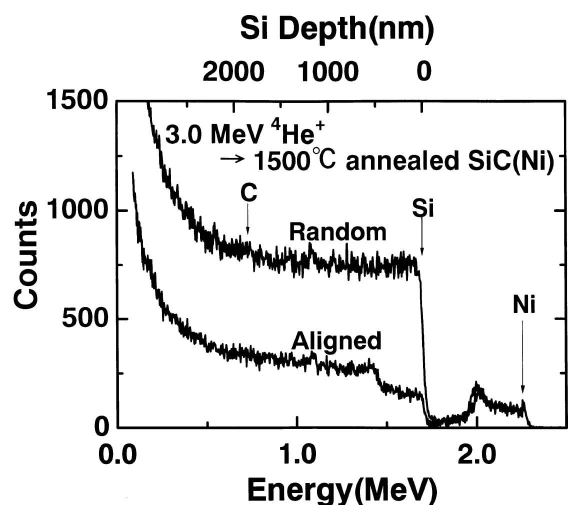

Fig. 4. Aligned and random backscattering spectra of 3.0 MeV $^{4}He^{+}$ ions from α-SiC(0 0 0 1) crystal implanted with 1.0 MeV Ni atoms of a dose of 1.8×10^{17} cm^{-2} at room temperature after thermal annealing of 1500°C and 2 h.

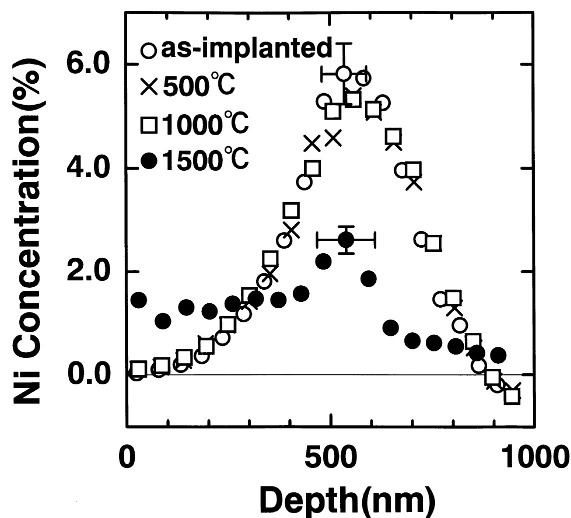

Fig. 5. Depth distributions of Ni atoms in α-SiC as implanted (○), and after 500°C (×), 100°C (□) and 1500°C (■) annealing. The 1.0 MeV Ni atoms were implanted with a dose of 1.8×10^{17} cm^{-2} at room temperature.

SEM photographs showed that the surfaces of the annealed samples with highest ion dose were not so smooth as those of lower dose ones and virgin samples due to the heavy implantation of Ni atoms.

RBS-C spectra and Fig. 5 show that the implanted Ni atoms distribute randomly in α-SiC and have an approximately Gaussian profile with a maximum concentration of 6.0 at.% at the depth of 540 nm with a FWHM of 320 nm for the highest dose as-implanted sample. During the 1500°C annealing, the Ni atoms start to diffuse to the surface, and then distribute like a trapezoid profile except a small peak at 540 nm as observed in the case of the defects profile. This indicates that a region with a relatively high Ni concentration and a defect layer with a high defect concentration exists at the depth of near 540 nm in the recrystallized sample. These defects may form correlated defects with Ni atoms in this region. It is found that the heavily damaged sample was also recrystallized completely after the second 1500°C annealing.

Acknowledgements

The authors wish to thank Dr Aruga for the E-DEP-1 calculation and Mr. Nakae for his assistance during this work. This work has been supported in part by the Universities JAERI Joint Research Project for the Advanced Radiation Research.

References

[1] R.R. Hart, H.L. Dunlap, O.J. Marsh, Radiat. Eff. 9 (1971) 261.
[2] O.J. Marsh, Silicon Carbide-1973, University of South Carolina, Columbia, 1974, p. 471.
[3] R.B. Wright, D.M. Gruen, Radiat. Eff. 33 (1977) 133.
[4] J.M. Williams, C.J. McHargue, B.R. Appleton, Nucl. Instrum. Meth. 209/210 (1983) 317.
[5] J.A. Spitznagel, S. Wood, W.J. Choyke, N.J. Doyle, J. Bradshaw, S.G. Fishman, Nucl. Instrum. Meth. B 16 (1986) 237.
[6] C.J. McHargue, G.C. Farlow, G.M. Begun, J.M. Williams, C.W. White, B.R. Appleton, P.S. Sklad, P. Angelini, Nucl. Instrum. Meth. B 16 (1986) 212.
[7] H.G. Bohn, J.M. Williams, C.J. McHargue, G.M. Begun, J. Mater. Res. 2 (1987) 107.
[8] N.G. Chechenin, K.K. Bourdelle, A.V. Suvorov, Nucl. Instrum. Meth. B 48 (1990) 235.
[9] A. Föhl, R.M. Emrick, H.D. Carstanjen, Nucl. Instrum. Meth. B 65 (1992) 335.
[10] N.G. Chechenin, K.K. Bourdelle, A.V. Suvorov, A.X. Kastilio-Vitloch, Nucl. Instrum. Meth. B 65 (1992) 341.
[11] L.L. Horton, J. Bentley, L. Romana, A. Perez, C.J. McHargue, J.C. McCallum, Nucl. Instrum. Meth. B 65 (1992) 345.
[12] N. Shimatani, K. Kawatsura, S. Arai, T. Shiono, Y. Horino, Y. Mokuno, K. Fujii, H. Takeshita, S. Yamamoto, Y. Aoki, H. Naramoto, Nucl. Instrum. Meth. B 91 (1994) 529.
[13] N. Shimatani, K. Kawatsura, R. Takahashi, A. Nishihata, S. Arai, Y. Aoki, S. Yamamoto, H. Takeshita, H. Naramoto, Y. Horino, Y. Mokuno, K. Fujii, Silicon Carbide and Related Materials 1995, IOP, Bristol, 1996, p. 1063.
[14] W.-K. Chu, J.W. Mayer, M.-A. Nicolet, Backscattering Spectrometry, Academic Press, New York, 1978.
[15] K. Kawatsura et al., private communication.